9th CIGRE Southern Africa
Regional Conference
1st – 4th October 2019
Johannesburg, South Africa

Electroluminescence Imaging of Photovoltaic Modules

M.T Malefafana[1,2], L. Pratt[2,*], M. Basappa Ayanna[2], K. Roro[2]
[1]Tshwane University of Technology, Department of Physics, Pretoria, South Africa
[2]Council for Scientific and Industrial Research (CSIR), South Africa

SUMMARY

Electroluminescence (EL) imaging is a non-destructive characterization technique used widely across the solar PV industry. Similar to an x-ray image, the EL image allows the analyst to peer inside the PV module and see features that are otherwise impossible to view with the naked eye. Those features include grain boundaries, interconnects, defects in the silicon, cracked cells and inactive cell areas.

The integrity of the solar cells is critical because the cells are the generators that convert solar radiation into direct current electrical energy. Therefore, EL is used at a number of points in the supply chain to minimize the negative impact from cracked cells and inactive areas. EL images are collected at the factory during manufacturing processes, quality assurance batch testing, routine operations and maintenance as well as during failure analysis of fielded modules in real world conditions.

In this paper, the basic techniques used to capture EL images at the CSIR are presented. Some of the typical features that can be seen on multi-crystalline silicon and mono-crystalline silicon photovoltaic (PV) modules, as well as bi-facial modules are presented. Two case studies have been analyzed as part of the failure analysis. One shows the impact that a handling mishap can have on the integrity of the solar cells. The second case study shows the use of EL, infrared thermography and the electrical characterization to investigate a module with burned back sheet.

KEYWORDS

EL, Electroluminescence, PV module, Defects, Microcracks, Hotspots

[*]**Corresponding Author's Email**: lpratt@csir.co.za

1 INTRODUCTION

Electroluminescence (EL) imaging of wafer-based photovoltaic (PV) modules is an effective technique to detect defects in solar modules (Jahn et al., 2018) (Crozier et al., 2012). Under normal operating conditions, a PV module absorbs light energy and converts some of that light into electrical energy. During EL imaging, the PV module absorbs electrical energy and converts some of the electrical energy in to light energy. This occurs as a result of recombination of minority charged carriers through the p-n junction causing light emission. Crystalline silicon solar cells emit radiation in the infrared (IR) region (950-1300 nm) of the electromagnetic spectrum (Petraglia and Nardone, 2011). This radiation can be detected by a cooled silicon charge-coupled device camera since it is not visible to the human eye. The optical image can then be analysed by humans and machine learning algorithms to detect cracks, inactive areas, and other defects in solar cell (Gopalakrishna et al., 2018) (Deitsch et al., 2018).

In this paper, we will present the EL test procedure, some typical EL images of standard silicon wafer-based PV modules and results of an EL inspection on a failed module from the CSIR dual-axis PV plant.

1.1 PURPOSE

EL images are essential for detecting defects in PV modules including broken cells, micro-cracks, black edges, dark / bright spots and cells. These defects can occur anytime during the lifetime of the module from manufacturing, handling, shipping, installation, and maintenance. EL is also used to detect Potential Induced degradation (PID) in which PV module performance degrades due to stresses caused by the string level system voltage (Hacke et al., 2011). The defects may have a significant effect on the lifetime and performance of the PV module, so screening based on EL imaging occurs at several stages along the supply chain to reduce the risk from cracked cells. EL images are collected at the PV manufacturing plant, during quality assurance testing, module certification and failure analysis.

2 CSIR INDOOR EL SETUP

The CSIR EL lab includes a dark room, an EL camera and a direct current (DC) power supply (Figure 2.1). The camera is mounted on an adjustable tripod stand and connected by a USB cable to a PC with a digiCamControl software. The CSIR uses a modified Nikon digital single lens reflex (DSLR) camera, which provides reasonable quality at a low price. The DC power supply is connected to the PV module and provides the electrical bias at a current equal to the PV module short circuit rating as stated on the nameplate.

Figure 2.1 Indoor EL imaging lab at the CSIR

There are alternative hardware configurations for EL imaging and the IEA-PVPS T13-10:2018 report provides detailed comparison of the many options (Jahn et al., 2018). EL images can be taken on modules with a single shot or several smaller shots stitched together for higher quality. They can be taken in dark rooms as at the CSIR or in the field at night or during twilight hours. Mobile PV labs can be brought to the PV plant so that modules can be imaged in a dark room without the risk and cost associated with transportation. Hardware is also available so that EL images of modules and strings can be taken during the day without removing the modules from the mounting rails. In all cases, however, the module or string must be disconnected from the system so that an electrical bias can be applied.

3 PERFORMING AN EL INSPECTION

EL image inspection is a type of non-destructive testing performed under dark conditions for high-resolution images with cooled detectors for high sensitivity. The detectors are sensitive to the near IR radiation emitted by the PV module. Filters on the camera lens may be used to help cut light of unwanted wavelengths from being detected. A 950 nm long-pass filter is used for imaging EL on modules with silicon cells.

EL imaging begins with the artificial generation and recording of an emission spectrum that is outside the visible range of 380 to 740 nm. Figure 3.1 shows the emission spectrum (blue profiles) and the sensitivity of various detectors (green profiles).

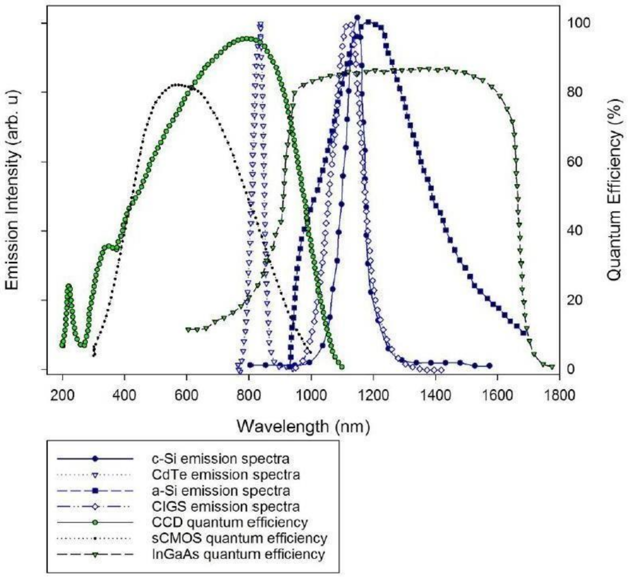

Figure 3.1 EL emission intensity of various PV materials and quantum efficiency of various detectors.

Source: (Jahn et al., 2018)

To increase the quality of the EL image, the focal ratio is set to the smaller f-number = 1/8 which corresponds to the largest aperture so that as much light is gathered as possible. The exposure time is set to 30 seconds. The sensitivity is controlled by the ISO setting. For long exposure times, ISO is set to 100 and for short exposure times it is set to 500. The sensitivity and exposure time must be balanced to avoid over-exposure. The focus modes are switched from manual to auto-focus when taking an image with the camera and manual when using the digiCamControl software so that it is easy to adjust the ISO and exposure time using the computer.

Powering the PV module is crucial since the emission intensity depends on the applied voltage. The power supply used must be capable of providing the needed power to allow the cell to emit an adequate amount of EL radiation (Petraglia and Nardone, 2011). Depending on the type of PV module, the output voltage on the power supply must be approximately equal to the open circuit voltage (V_{oc}) of that particular PV module. At the CSIR, the standard operating procedure follows:

1. Place the PV module in the test lab
2. Clean the module of any visible smears that might block emission
3. Forward bias the PV module with rated Isc rated current
4. Switch ON the camera and PC and make sure that the digiCamControl software is running in order to take an image from the PC.
5. Turn OFF the lights and close other sources of light so that the lab is dark to obtain high-resolution images.
6. Choose ‘LV' option in the ‘video capture method' for focusing and pre-processing of the EL image.
7. Close the ‘LV' and capture the image.
8. Turn OFF the power supply immediately and switch ON the lights.

The recorded image collected by the sensor in the near IR spectrum is translated by the camera to a distribution of intensity across the surface of PV module or string of modules which can then be viewed as an image on the screen. The relative intensity is then analysed to detect cracks, inactive cell area and many other features. The EL image is processed so that every detail of the defects may be identified for characterization and analysis. For the processing of the image, Gimp manipulation software and Python programming software are used. With Gimp, a perspective layout adjustments and cropping out of unwanted area is done so that only the EL image (area of interest) is viewed. We are developing image processing scripts in Python for routine, automated analysis. The scripts are also being developed for perspective layout, brightness and contrast optimization, pre- and post-mechanical load test comparisons, and ultimately crack detection.

4 RESULTS

4.1 Initial EL Images of Mono and Multi-Crystalline Silicon Modules

Several EL images are presented below to highlight some of the normal features that can be “seen” with a standard EL image of various PV technologies. Figure 4.1 shows a typical multi-crystalline wafer based PV module (internal CSIR ID = 18000-28). This module consists of 60 square cells interconnected with three ribbons, which can also be deduced from an optical image. The EL image also shows the grain boundaries caused by different crystal orientations that evolve from the ingot production and from this image, one can deduce that some cells in this module were made from wafers cut from the same block of silicon. For example, the three cells highlighted in Figure 4.1 were likely cut from the same block because they show the same grain boundary pattern as one another. Grain boundaries can sometimes be seen with the naked eye, but the anti-reflective coatings on the cells can make them difficult to distinguish. There are other examples of matching wafers in the image below, and sometimes the match can only be made by flipping or rotating one cell or the other.

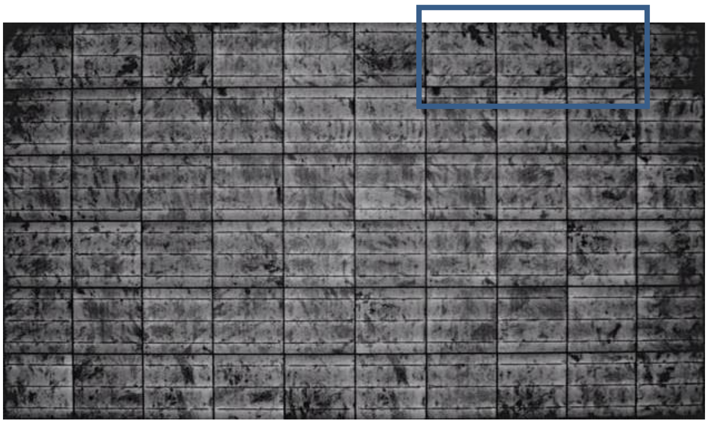

Figure 4.1 EL image of multi-crystalline module with square cells, grain boundaries and three interconnect ribbons.

Figure 4.2 shows a typical mono-crystalline module (18000-29). This module consists of 60 pseudo-square cells, three interconnect ribbons, and no grain boundaries. This image also shows four visibly cracked cells (diagonally oriented lines) and defects associated with the growth of the ingot (dark blobs in the centre of the cells).

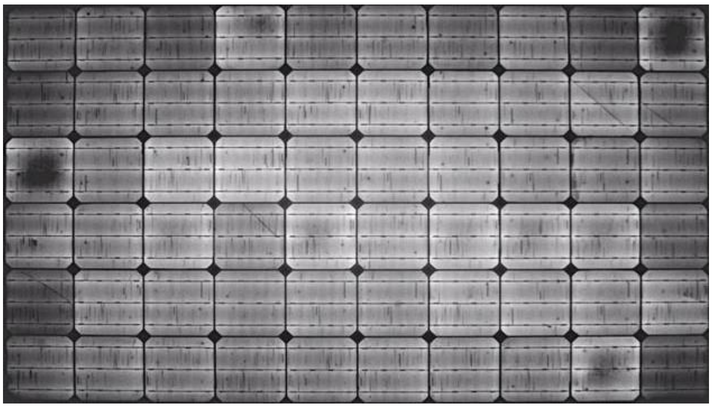

Figure 4.2 EL image of mono-crystalline module with pseudo-square cells, three interconnect ribbons, and no grain boundaries

Figure 4.3 and 4.4 shows the front and back side of a bifacial module made from mono-crystalline cells and five interconnect ribbons (18000-51). Dark spots in the cells can be seen at the same location from the front and back side of the module, after rotating the image accordingly. The backside image clearly shows the junction box and the nameplate label to a lesser extent. The image from the backside is also slightly darker overall, so it's tempting to conclude the efficiency on the backside is lower. While the backside efficiency of bifacial solar PV module is lower than the front side, it would be wrong to conclude this from the EL image. The overall intensity level in the image may be a function of the camera settings, the power supply settings, and the post-processing.

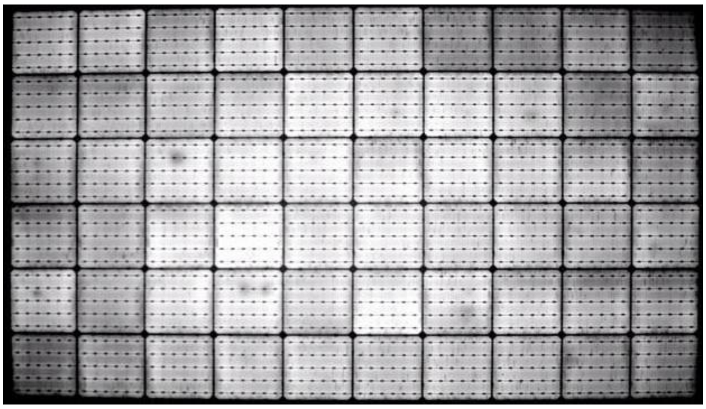

Figure 4.3 EL image of Bifacial mono crystalline module: front side

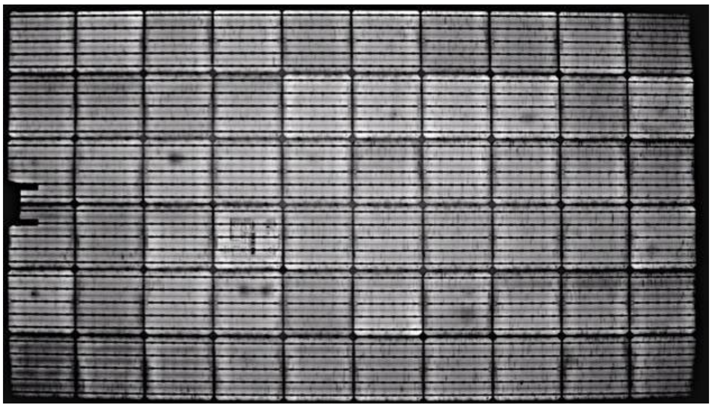

Figure 4.4 EL image of Bifacial mono crystalline module: back side

4.2 Qualitative Analysis of EL Images

Microcracks can have disproportionately large impacts on module performance when the microcracks lead to inactive areas greater than 8-10% of the cell area (Köntges et al., 2010). Figure 4.5 shows a mono-crystalline module with a number of cells impacted by cracks (18000-22). The cells with line cracks will generally not reduce performance significantly, but the cells with large black areas highlight inactive areas. The inactive areas can lead to reduced cell current which then reduces the overall substring current. Line cracks also have the potential to grow and create inactive areas over time, depending on the orientation of the crack and additional stress that might occur on the module. For instance, the original image of this module on the bottom left hand side showed far fewer cracks and smaller inactive areas. After a handling mishap, the additional stress caused new cracks to form, minor line cracks to grow and inactive regions to darken (image on the bottom right hand side). The module was leaning against the wall in portrait orientation and fell over on to the floor.

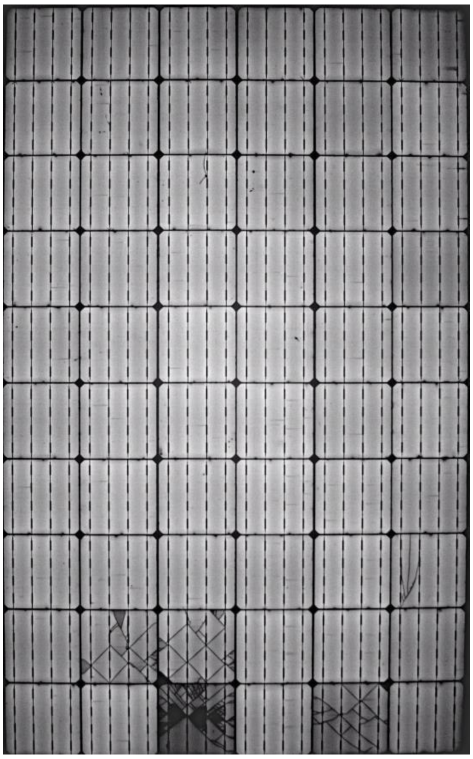

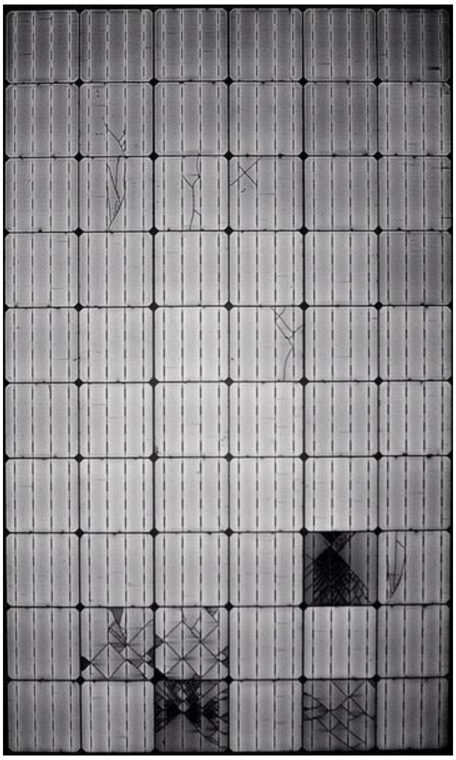

Figure 4.5 EL image of monocrystalline PV module with cracked cells and inactive areas as received (left) and post handling mishap (right)

Figure 4.6 shows an EL image of a mono-crystalline module as received (18000-32). The typical interconnect ribbons does not exist, and instead the 'dog-bone' type interconnect can be seen in the vertical space between two adjacent cells which is typical of a back contact module. In this example, there are a number of cracked cells and dark regions. The dark cells likely have a negative impact on performance. Module power measured 2% lower on this module compared to a similar module (18000-31) from the same batch with a cleaner EL image.

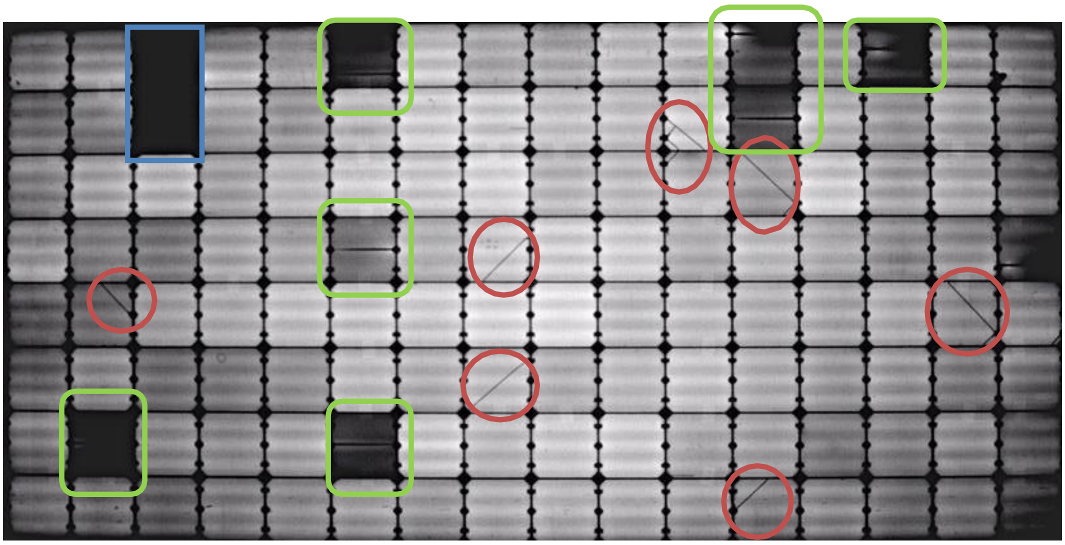

Figure 4.6 EL image with defects

Figure 4.7 shows an EL image from a module that exhibited hotspot burn marks on the backsheet (18012-01). It is suspected the damage is from a nearby lightning strike. The module was removed from the CSIR dual axis PV plant and investigated further with EL, hotspot per IEC 61215-2:2016, and electrical measurements. The hotspot endurance test is conducted during certification testing to ensure modules are designed and built in a manner to minimize the hotspot impact due to a number of conditions including faulty cells. An experimental hotspot endurance test of was carried out on good substrings to see if we could induce additional burn marks. By analysing the shaded IV curves in Figure 4.7, the cell in row 2, column 5 was identified as a potential low shunt resistance cell. The backsheet temperature did not exceed 150 °C during the hotspot endurance test on this cell, nor did it cause any burn mark. Based on this outcome, it's unlikely that the burn marks were caused by hotspots arising from defects in the cells or from poor manufacturing.

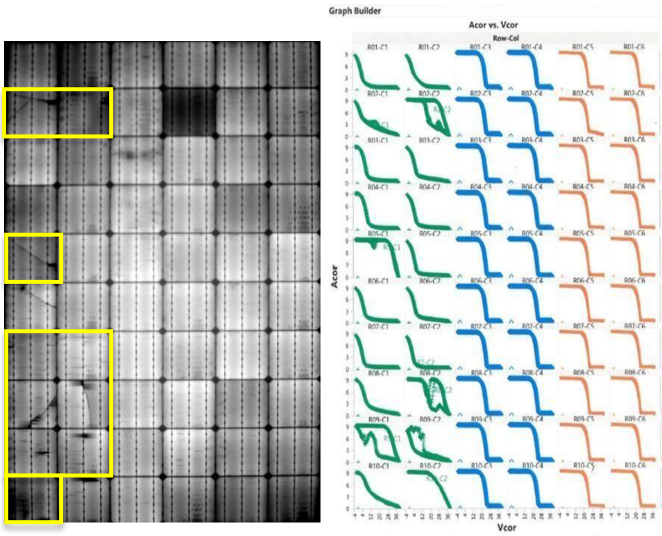

Figure 4.7 EL image and corresponding shaded cell IV curves.
Yellow squares indicate cells with burn marks on the backsheet

In the next step, the presence of burn marks and cracked cells were correlated. Perhaps the cracked cells were arcing and creating excessive heat leading to the burn marks. The cracked cell in row 5, column 1 was subjected to the hotspot endurance test in the same method described above. This cracked cell was allowing full module power to pass through the cell during all three shaded cell IV curves. The backsheet temperature reached 160 °C during the hotspot endurance but failed to show any additional damage to the backsheet. Furthermore, the correlation between cracked cells and burn marks for this module was not statistically significant based on a contingency analysis of the 20 cells in the substring.

Further investigation confirmed that the bypass diode in the faulty substring had failed in open circuit. The shaded IV curves confirm the proper function of the bypass diodes for the substring in the centre and right side of the module, and abnormal operation for the bypass diode in the substring on the left side. Post removal of the potting material in the junction box, the bypass diode bond was found to be debonded from the junction box connection point.

5 CONCLUSION

EL imaging is an integral part of silicon PV module characterization. EL images enable detection of cracks and inactive regions in the silicon solar cell that have been reported in the literature to result in performance degradation. Microcracks can increase in size and severity as a result of mishandling. Based on the analysis of one module substring with a faulty bypass circuit, no correlation was established between cracked cells and backsheet burn marks.

BIBLIOGRAPHY

Deitsch, S., Christlein, V., Berger, S., Buerhop-Lutz, C., Maier, A., Gallwitz, F., Riess, C., 2018. Automatic Classification of Defective Photovoltaic Module Cells in Electroluminescence Images. ArXiv180702894 Cs.

Gopalakrishna, H., Yadav, R., Chan, E., Wu, J., TamizhMani, G., 2018. Durability evaluation of PV modules using image processing tools, in: Munday, J.N., Bermel, P., Kempe, M.D. (Eds.), New Concepts in Solar and Thermal Radiation Conversion and Reliability. Presented at the New Concepts in Solar and Thermal Radiation Conversion and Reliability, SPIE, San Diego, United States, p. 36. https://doi.org/10.1117/12.2322500

Hacke, P., Terwilliger, K., Smith, R., Glick, S., Pankow, J., Kempe, M., Bennett, S.K.I., Kloos, M., 2011. System voltage potential-induced degradation mechanisms in PV modules and methods for test, in: 2011 37th IEEE Photovoltaic Specialists Conference. Presented at the 2011 37th IEEE Photovoltaic Specialists Conference (PVSC), IEEE, Seattle, WA, USA, pp. 000814–000820. https://doi.org/10.1109/PVSC.2011.6186079

Jahn, U., Kontges, M., Parlevliet, D., Paggi, M., 2018. Review on IR and EL Imaging for PV Field Applications.

Köntges, M., Kunze, I., Kajari-Schröder, S., Breitenmoser, X., Bjørneklett, B., 2010. Quantifying the risk of power loss in PV modules due to micro cracks 9.

Petraglia, A., Nardone, V., 2011. Electroluminescence in photovoltaic cell. Phys. Educ. 46, 511–513. https://doi.org/10.1088/0031-9120/46/5/F01